JBC Papers in Press. Published on October 25, 2006 as Manuscript M607756200
The latest version is at http://www.jbc.org/cgi/doi/10.1074/jbc.M607756200

Trafficking and Assembly of the cold-sensitive TRPM8 channel

Isabell Erler, Dalia M.M. Al-Ansary, Ulrich Wissenbach, Thomas F.J. Wagner, Veit Flockerzi, Barbara A. Niemeyer*

From the Department of Pharmacology and Toxicology, University of Saarland, Medical Campus, 66421 Homburg, Germany

Running Title: TRPM8 trafficking and assembly

Address correspondence to: Barbara A. Niemeyer, Institut für Experimentelle und Klinische Pharmakologie und Toxikologie, Universität des Saarlandes, Geb. 46, 66421 Homburg, Germany, Tel.: +49 6841 1626405; Fax: +49 6841 1626402; E-mail: barbara.niemeyer@uniklinikum-saarland.de

TRPM channels are distinct from many other members of the TRP family in regard to their overall size (over 1000 amino acids), the lack of N-terminal Ankyrin like repeats and hydrophobicity predicitions that may allow for more than six transmembrane regions. Common to each TRPM member is a prominent C-terminal coiled-coil region. Here we show that TRPM8 channels assemble as multimers using the putative coiled-coil region within the intracellular C-terminus and that this assembly can be disturbed by a single point mutation within the coiled-coil region. This mutant neither gives rise to functional channels nor do its subunits interact or form protein complexes that correspond to a multimer. However, they are still transported to the plasma membrane. Furthermore, wild-type currents can be suppressed by expressing the membrane attached C-terminal region of TRPM8. To separate assembly from trafficking we investigated maturation of TRPM8 protein by identifying and mutating the relevant N-linked glycosylation site and show that glycosylation is neither essential for multimerization nor for transport to the plasma membrane per se, but appears to fascilitate efficient multimerization and transport.

Although the family of TRP ion channels has originally been defined by their homology to their seminal member, the *Drosophila* Transient Receptor Potential (TRP) channel (1,2), their 28 mammalian homologs have evolved into different subfamilies with very distinct characteristics and a range of different functions. Many members share only a very distant homology to the original TRP channel. Although members of one subfamily generally have certain structural motifs in common, e.g. six ankyrin repeat elements for the TRPV family (3-5), a C-terminal coiled-coil domain for the TRPM channels and the TRP box and TRP domain, which are loosely conserved in all mammalian TRPs except TRPP and TRPA, these elements do not necessarily confer a similar function. Binding of PIP2 to the TRP-domain, for example, appears to inhibit TRPV1 channels (6), but stimulates TRPM5, 7 and 8 as well as TRPV5 (7-9) (10). Certain sensing modalities such as thermosensation are also not restricted to one subfamily: Altering activity depending on temperature is utilized by TRPV1-4, but also by TRPM8 and TRPA1 and TRPM2 (for reviews see (11-13)). Here, an interchangeable specific region has been found within the intracellular C-terminus that allows TRPV1 and TRPM8 to sense temperature (14).

In analogy to voltage gated potassium channels it is thought that four subunits need to assemble to form a functional channel. Experimental evidence for tetramer formation exists for TRPV1, TRPV2 and TRPV5/6 (15-18).

Because there is hardly any structural motif besides the amino acids adjacent to the pore within S5, S6 and the TRP domain shortly downstream of S6 (19) that is conserved among all members, it is unlikely that there is a general mechanism of ion channel assembly that will apply to all. Although TRPM channels generally have long N- and C-termini, they lack ankyrin repeat structures that have been implicated to play a role in ion channel assembly for TRPV5/6 and TRPV4 channels(18,20,21). Common to all TRPM members is a prominent putative C-terminal coiled-coil region (Fig S1), but only in the case of TRPM8, this coiled-coil region is at the very end of the protein. Tsuruda et al (23)

showed by circular dichroism spectra that the secondary structure of a peptide encompassing the putative TRPM8 coiled coil region indeed forms a four-stranded coiled-coil that are able to form tetramers. For TRPM4, an N-terminal truncation (Δ177aa) but not a C-terminal truncation which deletes the coiled-coil region interacts with wild-type and exerts a dominant negative effect on TRPM4 function (22).

We have analyzed the domains within TRPM8 that are involved in assembling functional ion channels and delineate the role of N-linked glycosylation for subunit trafficking. We find that the very C-terminal domain of TRPM8 that has a high probability of forming a coiled-coil structure, is necessary for interaction of subunits with each other and that oligomerization can be disturbed by a single point mutation within the coiled-coil region. Moreover, a membrane anchored C-terminal domain can exert a dominant negative effect on wild-type subunits. Largely similar results concerning the role of the coiled-coil region in assembly of TRPM8 channels were obtained by Tsuruda et al. (23) just prior to submission of our results, although differences exist in the interpretation of trafficking events. To analyze trafficking and assembly mechanisms in more detail we also analyzed the role of N-linked glycosylation for channel assembly and trafficking. We have identified N934 as the only relevant attachment site for N-linked glycans and investigated in detail the effects of mutating this site.

EXPERIMENTAL PROCEDURES

Recombinant proteins and site-directed mutagenesis - All N-terminal EYFP tagged or C-terminal superecliptic pHluorin (SpH) (24) tagged constructs were obtained by inserting the appropriate phusion polymerase (NEB) amplified hTRPM8 (NM_024080) fragments either in frame with the EYFP coding sequence (pEYFP-C1, Clontech) or containing the consensus sequence for initiation of translation in vertebrates followed by a start ATG for cloning into a pCAGGS vector modified to include an EcoRV site followed by the SpH coding sequence. Constructs containing an N-terminal SpH tag were cloned into a modified pCAGGS vector that contains an EcoRV restriction site in frame and downstream of the SpH coding sequence lacking the stop codon. In some cases, transfer of restriction enzyme digested DNA was used to transfer inserts from one vector into the other. Purity and identity of plasmid DNA were verified by dye terminator sequencing (PerkinElmer). Site directed mutagenesis was performed using either pBTL-CT or pEYFP-TRPM8 vector as template, appropriate mutagenesis primers and PCR conditions according to the quickchange kit (Stratagene).

Electrophysiology - Patch-clamp recordings on single transfected (Fugene, Roche) HEK 293, TSA cells were performed 48 to 72 h or 72-96 h (HEK-TRPM8) after transfection as described (3). Pipette solution contained (mM): 140 aspartic acid, 10 EGTA, 10 NaCl, 1 $MgCl_2$, 10 Hepes (pH 7.2 with CsOH). Bath solution contained (mM): 140 NaCl, 10 CsCl, 2 KCl, 2 $MgCl_2$, 2 $CaCl_2$, 10 glucose, 10 Hepes (pH 7,4 with NaOH). After break-in and 80% series resistance compensation, whole cell currents were recorded every second by applying 100 msec voltage-clamp ramps from -120 mV to +70 mV from a holding potential of -60 mV. Currents were analyzed at -101 mV and either at +31 or + 51 mV ramp potential. When bath solution alone or 100 µM Menthol in standard bath solution was locally perfused over the recorded cell, only one cell per dish was measured to prevent desensitization of other cells. Currents (pA) were divided by the whole cell capacitance (pF). Data are given as mean ± SEM. Values were not corrected for liquid junction potentials. Cotransfections were performed with 0.8 µg EYFP-TRPM8 mixed with 1.2 µg of C-terminal constructs or 1.8 µg of TRPM8-ΔCT resulting in a ~2.3 fold excess over wild-type. Transfected cells were trypsinated and seeded at low density after 24 hours.

Co-immunprecipitation experiments - TRPM8 stable HEK 293 (TRPM8s) cells were transfected with TRPM8-SpH expression constructs, cultured for 48 h, washed once with PBS, treated with trypsin for 1 min, pooled after adding medium and centrifuged for 7 min at 1000 rpm (4°C), washed once with ice-cold PBS, centrifuged for 7 min at 1000 rpm and resuspended depending on the size of the cell pellets in 1 to 2 ml ice cold RIPA buffer (150 mM NaCl, 50 mM Tris-HCl pH 8.0, 0.5% sodiumdeoxycholate, 1% Nonidet P40, 0.1% SDS, 5 mM EDTA) with added protease inhibitors (1 µg/ml leupeptin, 0.1 mM PMSF, 1 mM pepstatin A or 1 µg/ml antipain, 0.3 µM aprotinin, 1 mM benzamidin). Cells were lysed by sequential pipetting through three different

gauge syringe-needles (0.7, 0.55, 0.4 i.d.). After lysis, 50 µl of the lysate was precipitated with trichloroacetic acid, washed with aceton and resuspended in loading buffer, the remaining lysate was centrifuged at 14000 rpm for 15 min at 4°C. Supernatants containing ~ 3mg of total protein were incubated for 2 h with 6 µg monoclonal anti-GFP antibody (Roche), then with added protein-G-sepharose beads at 4°C overnight. After 5 washes with RIPA buffer, beads were resuspended in loading buffer, treated for 3 min at 95°C, subjected to SDS-PAGE and analyzed by Western blot analysis.

Cell-surface biotinylation - Dishes with confluent transfected HEK, TSA or COS cells were harvested 48 h after transfection, washed and treated as described in (25). 900 µg protein was used as input for the avidin agarose beads. Controls included monitoring the input of TRPM8 protein as well as testing for the absence of calnexin (ER protein) in the avidin agarose precipitant. Westen blots were either probed with anti-GFP (1:500) or anti-TRPM8 (1:200) and pictures were taken with an LAS3000 cooled CCD camera. Non-saturated signals were quantitated using AIDA (raytest) software and the amount bound to avidin was divided by the total amount unbound.

Sedimentation by sucrose gradient centrifugation TSA cells transfected with EYFP-TRPM8 or EYFP-TRPM8-L1089P were harvested and microsomal proteins were isolated according to (26) and resuspended in 200 µl buffer (150 mM NaCl, 50 mM Tris-HCl, pH 8; 0.5% Na-deoxycholate, 5 mM EDTA, 10 % (v/v) glycerol, 1 µg/ml leupeptin, 0.1 mM PMSF, 1 mM pepstatin A). 1.3 mg total protein was loaded onto a continuous 15-25% sucrose gradient (in 20 mM TRIS, 5 mM EDTA, 0.1% Triton-X-100 and protease inhibitors as above; marker gradient was without 0.1% Triton-X-100) and subjected to 50000 rpm (NVT65) for 2h. 15 fractions at 690 µl were collected and 72 µl of each fraction in 5x Laemmli buffer was resolved with on SDS-PAGE gels and analyzed by immunoblotting. A parallel gradient was run with marker proteins thyroglobulin, ferritin, catalase, ß-glycosidase (Sigma), fractions were resolved on appropriate SDS-PAGE gels and stained with coomassie

Antibodies and Reagents - Polyclonal anti-TRPM8 (797) antibodies were generated against the terminal 24 amino acids of hTRPM8 in our laboratory and affinity purified and used at 1:200 or 1:150 for Western blots; monoclonal anti-GFP antibody (Roche) was used at 1:500 for Western blots, anti-IP3RIII antibody (Santa Cruz) was used at 1:100.

Bacterial-Two-Hybrid - Experiments were performed by using the Bacteriomatch two hybrid system II (Stratagene) with the following modifications: DNA encoding a bait or a target protein was cloned in frame into pTRG or the modified pBT vector (pBTL) containing a $(gly_4ser)_3$ linker. All constructs were sequenced. Electro-competent bacteria (Bacteriomatch two-hybrid system reporter strain, Stratagene) were thawed on ice and electroporated in the presence of 50 ng pTRG constructs and 50 ng pBTL constructs (BioRad 2,5 kV, 200Ω, 25 µF). After adding 1 ml SOC-medium, cells were incubated at 37° C under shaking (225 rpm) for 1,5 h, washed once with HIS drop-out media and adapted for 2h at 37° C under shaking in HIS drop-out media before plating. 200 µl bacterial culture were plated on selection plates (Stratagene, with 12.5 µg/ml tetracycline, 25 µg/ml chloramphenicol) either with or without 5 mM 3-AT and incubated at 37°C for 24 h. Interactions were detected by growth and number of colonies.

Stable cell lines and cell culture conditions - HEK 293 (CRL-1573, ATCC Manassas, VA) were maintained in minimal essential medium (MEM, Gibco) containing 10% fetal calf serum in a 37°C/5% CO_2 incubator and passaged by treatment with trypsin. hTRPM8 containing pCDNA3 vector was transfected into the cells by using the SuperFect Transfection reagent (Qiagen) and selected in the presence of 500 µg/ml Geneticin (Gibco). Surviving cells were isolated by cell sorting, subcloned and tested by Western blot for the presence of TRPM8 transcript and protein. For this study we used the clonal TRPM8 cell line M8A3 where indicated.

Deglycosylation experiments - 50µg protein of a microsomal membrane preparation (26) from HEK-TRPM8 cells were incubated for 2 h in the appropriate buffers following the instructions (NEB) either with or without EndoH or NGase F.

RESULTS

Identification of self-interacting sites

To identify interacting domains within the TRPM8 amino acid sequence, we analyzed protein-protein interactions within the presumed cytoplasmic tails using a bacterial-two-hybrid system (Bacteriomatch II®, Stratagene). Using the secondary structure prediction algorithm coils by Lupas (27), we found three weak putative coiled-coil domains within the N-terminal region and one very strong prediction of a coiled-coil domain at the very C-terminal region of the protein. As shown schematically in Fig. 1A, we divided the N-terminal region into three constructs that each contain one putative coiled-coil domain and tested these as well as range of short C-terminal domains for self-interaction with the two hybrid system. Fig. 1B shows the results of the two-hybrid screen: Strong protein-protein interaction can be found both for a distal N-terminal region that encompasses the third putative coiled-coil domain as well as for those C-terminal constructs that contain the complete C-terminal coiled-coil (CC) region (terminal 42 aa). Interestingly, a C-terminal construct that contains the full CC region but lacks 69 upstream amino acids (C2) is much less potent at initiating reporter gene activity than the full C-terminal region or the construct that lacks only 29 upstream amino acids (C4), which may point towards a role of the relatively hydrophobic region between amino acids 1007 and 1047 in stabilizing the interaction.

To confirm protein interactions in a more native environment, we made use of a HEK cell line that stably expresses functional TRPM8. We transiently transfected either a full length TRPM8 construct tagged with a C-terminal superecliptic pH-sensitive GFP (wt-SpH, (24)) or different deletion constructs into this cell line (Fig 2A). Cell-lysates were harvested after 48 h and incubated with anti-GFP antibody. After precipitation of the GFP antibody we checked for the presence of the untagged wild-type TRPM8 in the Sepharose G bound fraction. As seen in Fig. 2B, the GFP tagged TRPM8 that is also detected by the anti-TRPM8 antibody (see double bands at ~ 150 kDa, indicative of post-translational modification, see below) is able to co-immunprecipitate the untagged wild-type protein (double bands at ~ 120 kDa). However, neither a short N-terminal construct nor the full length N-terminal region with its three putative weak coiled-coil regions is able to co-precipitate wild-type TRPM8. A third construct that contains the entire N-terminal region in addition to the six putative transmembrane domains but lacks the short intracellular C-terminal region shows an extremely reduced interaction with TRPM8. Equal levels of bound fusionprotein were checked by reprobing the Western blots with anti-GFP antibody and by checking the input for unbound untagged TRPM8. We also tested a C-terminal deletion with an intact TRP box (Δ 1007-1104), which is expressed, and found that it is also unable to interact (data not shown). These results together with the results of the two-hybrid screen point towards a dominant role of the very C-terminally located coiled-coil domain in channel tetramerization. To test this directly, we both deleted the last 18 amino acids and obtained non-functional channels and mutated a single hydrophobic amino acid within the coiled-coil region (Fig S1A). Leucine 1089 is in a central *a* position of the heptahelical repeat region of a coiled-coil structure and replacing this leucine by a proline theoretically breaks the helical structure and almost completely reduces the probability of this region to form a coiled-coil structure (27). We initally tested the mutant in the two hybrid screen and found that interaction is completely abolished (Fig. 2C). Introducing the mutation into full length SpH tagged TRPM8 also leads to a much reduced ability to co-precipitate wild type TRPM8 (Fig. 2D). Interestingly, the C-terminal SpH tagged L1089P mutant, but not a N-terminal EYFP tagged protein (data not shown) is not recognized by our TRPM8 antibody which might suggest that the mutation introduced a “kink” in the structure such that the epitope (aa 1081-1104) for the TRPM8 antibody is obscured by the C-terminal GFP. Nevertheless, the L1089P construct shows strong expression when detected by the anti-GFP antibody and is also efficiently precipitated by the GFP antibody (see input in Fig. 2D). In contrast to the wild-type SpH tagged construct (M8-SpH), the deletion constructs and the point mutant only appear at one distinct molecular weight and apparently are not posttranslationally modified (see also Fig. 4). Furthermore, neither the 18 amino acid deletion mutant nor the EYFP-TRPM8 L1089P mutant are able to form functional menthol inducible ion conducting channels (for EYFP-TRPM8Δ1088-1104, 0/5 cells showed a change of > 1 pA/pF in current after menthol perfusion, data not shown, for EYFP-TRPM8 L1089P 0/6 cells responded, see also Fig. 2E). To test whether this failure results from a lack of cell surface expression, we performed biotinylation experiments. Both the lower molecular and - to a much lower degree - the upper molecular weight form of wild-type

TRPM8 can be precipitated from the cell surface (Fig. 2F). Interestingly, the L1089P mutant is also biotinylated and retained by avidin-agarose, indicating that it is trafficked to the plasma membrane despite the fact that its oligomerization is greatly reduced. Cell surface expression of the TRPM8 L1089P mutant is 3-4 fold reduced compared to that of wild-type control (n= 3 independent experiments). The ER resident protein calnexin could not be detected in the fraction of proteins retained by avidin, indicating that only proteins exposed to the cell surface were biotinylated (Fig. 2F). This data would argue for the ability of TRPM8 monomers to still reach the plasma membrane. But are TRPM8 L1089P mutants really monomers and does the coiled-coil region at the very C-terminus of an ion channel indeed govern its subunit assembly and tetramerization? To test this directly, we separated channel complexes by sucrose density gradient centrifugation. Fig. 3A shows that while EYFP-TRPM8 protein shows a higher concentration in fractions resembling trimer (~450 kDa), tetramer (~600 kDa) and higher order complexes, the EYFP-TRPM8 L1089P mutant shows a clear shift to those fractions that concentrate proteins of molecular weights corresponding to the monomer (~150 kDa), thus confirming the much reduced ability of this mutant construct to interact with other monomers to form oligomeric channel complexes. The finding that some protein can be detected in each fraction is likely due to overloading of the gradient and disturbances during fractionation and is also seen for the marker proteins.

Expression of dominant-negative fragments

If the coiled-coil domain indeed is critical for tetramerization of TRPM8, we should be able to disturb TRPM8 function by coexpression of the coiled-coil domain without an intact pore region. When we co-expressed an N-terminally EYFP tagged TRPM8 C-terminal domain (amino acids 978-1104, CT) together with the full length channel, we saw a reduction in the menthol inducible currents upon coexpression ($p<0.05$ for outward currents, Fig. 3B) compared to cells cotransfected with the EYFP vector alone. Because the coiled-coil domain resides at the very C-terminal region of the protein and is not very distant from the last hydrophobic domain, we reasoned that a hydrophobic anchor may be necessary for an efficient interaction. We therefore extended the amino-acid sequence to include the sixth predicted transmembrane domain of TRPM8. This N-terminally EYFP tagged construct covered amino acids 921-1104 (TM6-CT), and efficiently suppressed menthol induced currents after coexpression with wild-type TRPM8 (Fig. 3B). This dominant-negative effect was partly reversible when amino acids 1088 to 1104 were deleted (TM6-CTΔ1088-1104, Fig. 3B). Because the effects are not fully reversible, it is possible that there is an upstream interaction site that is still functional. However, we could not detect a dominant-negative effect upon coexpression of wild-type with EYFP-TRPM8 Δ 921-1104 (Δ menthol: -99 ± 26 and 483 ± 114 pA/pF, n=5) or upon coexpression with EYFP-TRPM8 L1089P (-85 ±15 and 324 ± 62 pA/pF, n=8).

Because menthol induced currents are quite variable and it is difficult to control for effective cotransformation, we also expressed potential dominant-negative constructs in the stable TRPM8 cell line. Fig. 3C shows that expression of CT alone does not reduce menthol responses when compared to untransfected control (wt), but TM6-CT again is very effective in suppressing TRPM8 currents (Fig. 3C). Introducing the L1089P mutation into TM6-CT was able to reverse its dominant-negative effect in the stable cell line (Fig. 3C), which confirms that the coiled-coil interaction is indeed necessary for the dominant-negative effect and that other interaction sites are not as effective without an intact CC region. As also seen for the coexpression, expression of full length EYFP-TRPM8 L1089P does not have a dominant-negative effect (Fig. 3C). Differences between the effects of CT alone upon coexpression or expression in the stable cell line could be due to its inability to interfere with exisisting complexes

To confirm that TM6-CT, but not the CT alone can interact with wild-type TRPM8, we performed co-immunprecipitation experiments in the TRPM8-HEK cell line. In order to precipitate the constructs, we had to swap the tag, as the EYFP tag is not efficiently precipitated by the anti-GFP antibody. Construct TM6-CT* was N-terminally extendend to the next endogenous methionine residue (aa 911-1104) and included a C-terminal SpH tag (TM6-CT*), as did the CT construct. As we found in two independent transfections, TM6-CT* (also SpH-TM6-CT) but not CT-SpH was able to interact with wild-type TRPM8 (Fig. 3D). Interestingly, TM6-CT* only precipitated the non- and core-glycosylated form of TRPM8 (see below). Because our input control of TM6-CT* showed signals at two

apparent molecular weights, we tested if mutation of the glycosylation site eliminated the upper band. Fig. 3E shows the double band for TM6-CT*, but not for N934Q-TM6-CT*, confirming that the upper band corresponds to a complex glycosylated form (see below).

Glycosylation of TRPM8

Because we can clearly detect both the tagged and the untagged TRPM8 immunreactive proteins at two distinct molecular weights (i.e. Fig 2D), the higher molecular weight form is likely to correspond to the mature glycosylated protein. To test this, we isolated microsomal membranes from the TRPM8-HEK cell line and incubated these membranes either with endoglycosidase H (EndoH), which cleaves high mannose type sugars of ER resident transmembrane proteins, or with N-glycosidase F (NGaseF). As shown in Fig. 4A, the upper molecular weight band disappeared upon treatment with NGaseF but not upon treatment with EndoH, illustrating that these protein bands represent complex glycosylated TRPM8. To investigate the role of glycosylation for function and trafficking of TRPM8, we mutated both putative extracellular sites for N-linked glycosylation N821 and N934 (Fig. 4B). Residue N821 resides within the extracellular linker between the predicted TM3 and TM4; because efficient glycosylation requires a distance of at least 10 amino acids from the downstream transmembrane domain (28) it is unlikely that this asparagine residue is glycosylated. Indeed, analyzing lysates from cells expressing the TRPM8-N821Q mutant we found no apparent difference in the amount of glycosylated protein (Fig. 4C) or in the ability of this construct to form functional channels (data not shown). However, replacing the asparagines residue at position 934 by glutamine (N934Q) leads to disappearance of the complex glycosylated form of the protein (Fig. 4C). Asparagine at position 934 is located in the extracellular loop between TM5 and TM6 presumably in close proximity to the selectivity filter of the pore loop. By looking at TRPM8 glycosylation patterns we noticed that the relative percentage of complex-glycosylated protein compared to non/core-glycosylated form is less for transiently expressed fusionproteins (Fig. 4C) than for stably expressed proteins (compare Fig. 4A). This observation may indicate that the transiently expressed proteins have not reached full maturation after 48h.

To investigate whether N-glycosylation is essential for exit from the Golgi and for transport to the plasma membrane, we performed cell surface biotinylation in HEK cells expressing the TRPM8-N934Q mutant. Biotinylated proteins were retrieved from cell lysates by avidin agarose, resolved by SDS-PAGE and detected by Westernblot. Unglycosylated TRPM8 protein is clearly retained by avidin, indicating that an essential portion of the protein reaches the plasma membrane. Compared to wild-type TRPM8, about 2-3 fold less TRPM8-N934Q is biotinylated (3 independent experiments) but N-glycosylation is clearly not essential for exit from the Golgi (Fig. 4D). Because Glycosylation can have a local effect on protein folding which may depend on the environment of the N-linked glycosylation site (29,30), we introduced a second point mutation between N934 and TM6 that replaces the basic histidine at position +12 by an asparagine (H946N). Although the TRPM8-H946N mutant alone does not alter the glycosylation pattern (data not shown), the presence of both mutations leads to an almost complete disappearance of the mutated protein from the plasma membrane (Fig. 4D). We tested the ability of the double mutant to co-precipitate with wild-type TRPM8 subunits and found that although the construct is expressed and binds to the anti-GFP antibody, it fails to interact with wild type subunits (data not shown). Most likely, the double mutation results in a protein that is misfolded and misrouted.

Functional analysis of Glycosylation site mutants

To test whether unglycosylated proteins can still form functional tetramers, we recorded menthol induced current changes from wild-type and mutant constructs. Cells were stimulated by 100 µM Menthol and currents were analyzed at -101 mV and +32 mV ramp potentials. Shown in Fig. 5A is a time course of inward and outward menthol induced currents of EYFP-TRPM8 (black) and EYFP-TRPM8 N934Q (gray) expressing cells. Figure 5B shows sample current-voltage relationships of wild-type and mutant after stimulation with 100 µM menthol. Concomitant to the reduced surface expression, N934Q mutants show menthol induced currents that are significantly smaller than wild-type, but show no obvious alteration in the shape of the current-voltage relationship. Statistical analysis of menthol induced changes in current densities is shown in Fig. 5C: N934Q mutants display inward and outward currents that are reduced ~ 4

fold compared to wild-type. As expected from the absence at the plasma membrane, the N934Q_H946N double mutant does not show detectable menthol inducible current changes (Fig. 5C). The failure of the double mutant to respond to menthol is not due to the H946N mutation as this mutant shows menthol induced current changes that are not significantly different from wild-type (Fig. 5C).

Having the N934Q mutant at hand we investigated whether unglycosylated subunits only interact with non- or core glycosylated TRPM8 subunits and possibly prevent the heteromeric complex from becoming glycosylated. Fig. 5D shows the co-immunprecipitation of non-glycosylatable TRPM8 (TRPM8 N934Q-SpH) with untagged wild-type TRPM8. Although the non/core-glycosylated form of the endogenous TRPM8 clearly interacts more strongly, unglycosylated subunits can also interact with complex glycosylated subunits, suggesting that either coassembly takes place in the ER and some wild-type subunits of the heteromeric mutant/wild-type complex become glycosylated and can be co-precipitated or that interaction of subunits is primarily a stochastic process that takes place in the ER but also in latter compartments such as the Golgi and possibly also in the plasma membrane.

DISCUSSION

In this study we provide evidence that a C-terminal coiled-coil region can drive tetramerization of TRPM8 channels. Analysis of protein interactions using a bacterial two hybrid assay point towards a strong protein interaction within the C-terminal coiled-coil region, but also to a role of a weaker coiled-coil region within the N-terminal region. While a strong C-terminal coiled coil region can be found in all members of the TRPM subfamily (Fig. S1A), N-terminal coiled-coil regions are not a general feature of TRPM channels and only in the case of TRPM5 a four heptad coiled-coil can be found (Fig. S1 B). Coimmunprecipitation studies confirmed the dominant role of the C-terminal coiled-coil, the putative N-terminal site cannot rescue interaction when the C-terminal domain is either deleted or a helix breaking point mutation (L1089P) is introduced into the center of the C-terminal coiled-coil. Moreover, the N-terminal coiled-coil (aa 594-628) contains a higher percentage (9.5 %) of alanines within positions *a* or *d* of the heptahelical repeat sequence which favors dimer over tetramer formation compared to the C-terminal CC region with only 2.6 % alanines favoring a tetramer (31,32). It might be possible that the N-terminal site plays a “prezippering” or stabilizing role in vivo.

Deletion of the last 18 amino acids or introduction of the L1089P mutation within a central *a* position of the C-terminal CC region leads to non-functional channels. EYFP-TRPM8 proteins co-assemble as trimers, tetramers and possibly as even higher molecular weight complexes as seen on sucrose density gradients and the L1089P mutation is sufficient to prevent most of this assembly. Confirming a critical role of the CC region for channel formation is the finding that expression of a membrane anchored C-terminal region is able to suppress TRPM8 mediated currents and interfering with the CC domain in the dominant-negative construct reverses its effects in the stable cell line. However, it is possible that secondary interaction sites exist that are more critical for the *de novo* synthesis. Our results come to a similar conclusion concerning an important role of the coiled-coil domain for the assembly role of TRPM8 as Tsuruda et al. (23), although we do not think that the coiled-coil region is solely responsible for assembly of other TRPM members (unpublished data). However, Tsuruda et al. argue that the dominant-negative effects of the membrane anchored CC are due to the reduction in complex glycosylated TRPM8 subunits and that the remaining function is likely due to some remaining glycosylated wildtype subunits that are difficult to detect on Western blots. Our results differ concerning the potential role of N-linked glycosylation. We identified asparagine 934 as the only acceptor site for N-linked glycans. TRPM8 subunits with a mutated glycosylation site (N934Q) do not show complex glycosylation. However, neither transport to the plasma membrane nor the ability to form functional channels is abolished. This differs from the role of N-linked glycans for trafficking of Eag1 potassium channels (33), HCN channels (34), Aquaporin-2 (35) among others. Interestingly, in the case of TRPV5, removal of extracellular glycans activates and stabilizes the protein at the surface (36).

In TRPM8, N-linked glycosylation takes place in the extracellular loop between TM5 and TM6 which also contains the putative pore region and selectivity filter (37). Analysis of potential N-linked glycosylation sites also revealed a site within the TM5-TM6 region for TRPM2, the closest relative of TRPM8, but also for TRPM4

and TRPM5, but not for TRPM3, TRPM6 and TRPM7. In each case, the putative glycosylation sites are downstream of the presumed selectivity filter and in the case of TRPM2 and TRPM8 are flanked by two cysteins. Correct folding of the pore region is critical not only for function but also for recognition by the oligosaccharyl-transferases. The discrepancy between the 2 to 3 fold reduction in surface expression compared to a ~ 4 fold reduction in menthol induced current density could be due to a decrease in open probability of the N934Q mutant. Although the N934Q mutant is still trafficked and functional, a second mutation 12 amino acids downstream destabilizes the region in such a way that subunits are unable to multimerize or traffic to the plasma membrane. This suggests that although tetramerization is likely to be initiated in the ER, correct folding and mature glycosylation of TM5-TM6 linker region in the Golgi stabilizes the tetramers. Because N934Q mutants can interact with complex glycosylated subunits, not all subunits of the tetramer need to be glycosylated or interactions may also happen in post-ER compartments. However, subunits that are unable to interact, such as the TRPM8-L1089P mutant or the C-terminal deletion mutants are not glycosylated, although a fraction of the subunits are still trafficked to the plasma membrane. This suggests that while subunit interactions are likely to be a stochastic process that takes place primarily in the ER, but possibly also in the Golgi, Oligosaccharyltransferases only glycosylate one or more subunits of a tetramer. Upon heteromultimerization with dominant-negative constructs, the physiological effects are likely due to a reduction of total protein. Because only a fraction of total TRPM8 protein shows complex glycosylation, a reduction in total protein could result in loss of detection of the glycosylated form as seen by Tsuruda et al (23). However, neither oligomerization nor glycosylation is a prerequisite for trafficking to the plasma membrane. Because surface expression is nevertheless reduced in the L1089P CC mutant as well as in the N934Q glycosylation site mutant, tetramerization and mature glycosylation either increase the efficiency of transport to the membrane and/or prolong the stability of TRPM8 molecules once they reach the plasma membrane. Accordingly, N934Q mutant subunits still form functional channels with menthol inducible current densities that are smaller than wild-type.

REFERENCES

1. Montell, C., and Rubin, G. M. (1989) *Neuron* 2(4), 1313-1323.
2. Hardie, R. C., and Minke, B. (1992) *Neuron* 8(4), 643-651.
3. Wissenbach, U., Niemeyer, B. A., Fixemer, T., Schneidewind, A., Trost, C., Cavalie, A., Reus, K., Meese, E., Bonkhoff, H., and Flockerzi, V. (2001) *J Biol Chem* 276(22), 19461-19468.
4. Jin, X., Touhey, J., and Gaudet, R. (2006) *J Biol Chem*
5. McCleverty, C. J., Koesema, E., Patapoutian, A., Lesley, S. A., and Kreusch, A. (2006) *Protein Sci*
6. Chuang, H. H., Prescott, E. D., Kong, H., Shields, S., Jordt, S. E., Basbaum, A. I., Chao, M. V., and Julius, D. (2001) *Nature* 411(6840), 957-962
7. Runnels, L. W., Yue, L., and Clapham, D. E. (2002) *Nat Cell Biol* 4(5), 329-336
8. Liu, D., and Liman, E. R. (2003) *Proc Natl Acad Sci U S A* 100(25), 15160-15165
9. Rohacs, T., Lopes, C. M., Michailidis, I., and Logothetis, D. E. (2005) *Nat Neurosci* 8(5), 626-634
10. Lee, J., Cha, S. K., Sun, T. J., and Huang, C. L. (2005) *J Gen Physiol* 126(5), 439-451
11. Liman, E. R. (2006) *Sci STKE* 2006(326), pe12
12. Tominaga, M., and Caterina, M. J. (2004) *J Neurobiol* 61(1), 3-12
13. Togashi, K., Hara, Y., Tominaga, T., Higashi, T., Konishi, Y., Mori, Y., and Tominaga, M. (2006) *Embo J* 25(9), 1804-1815
14. Brauchi, S., Orta, G., Salazar, M., Rosenmann, E., and Latorre, R. (2006) *J Neurosci* 26(18), 4835-4840

15. Kedei, N., Szabo, T., Lile, J. D., Treanor, J. J., Olah, Z., Iadarola, M. J., and Blumberg, P. M. (2001) *J Biol Chem* 276(30), 28613-28619
16. Jahnel, R., Dreger, M., Gillen, C., Bender, O., Kurreck, J., and Hucho, F. (2001) *Eur J Biochem* 268(21), 5489-5496
17. Hoenderop, J. G., Voets, T., Hoefs, S., Weidema, F., Prenen, J., Nilius, B., and Bindels, R. J. (2003) *Embo J* 22(4), 776-785.
18. Erler, I., Hirnet, D., Wissenbach, U., Flockerzi, V., and Niemeyer, B. A. (2004) *J Biol Chem* (33), 34456-34463
19. Montell, C. (2005) *Sci STKE* 2005(272), re3
20. Chang, Q., Gyftogianni, E., van de Graaf, S. F., Hoefs, S., Weidema, F. A., Bindels, R. J., and Hoenderop, J. G. (2004) *J Biol Chem* 279(52), 54304-54311
21. Arniges, M., Fernandez-Fernandez, J. M., Albrecht, N., Schaefer, M., and Valverde, M. A. (2006) *J Biol Chem* 281(3), 1580-1586
22. Launay, P., Cheng, H., Srivatsan, S., Penner, R., Fleig, A., and Kinet, J. P. (2004) *Science* 306(5700), 1374-1377
23. Tsuruda, P. R., Julius, D., and Minor, D. L., Jr. (2006) *Neuron* 51(2), 201-212
24. Miesenbock, G., De Angelis, D. A., and Rothman, J. E. (1998) *Nature* 394(6689), 192-195
25. Mery, L., Strauss, B., Dufour, J. F., Krause, K. H., and Hoth, M. (2002) *J Cell Sci* 115(Pt 17), 3497-3508
26. Lockwich, T. P., Liu, X., Singh, B. B., Jadlowiec, J., Weiland, S., and Ambudkar, I. S. (2000) *J Biol Chem* 275(16), 11934-11942
27. Lupas, A., Van Dyke, M., and Stock, J. (1991) *Science* 252(5010), 1162-1164
28. Nilsson, I., and von Heijne, G. (2000) *J Biol Chem* 275(23), 17338-17343
29. Mitra, N., Sinha, S., Ramya, T. N., and Surolia, A. (2006) *Trends Biochem Sci* 31(3), 156-163
30. Petrescu, A. J., Milac, A. L., Petrescu, S. M., Dwek, R. A., and Wormald, M. R. (2004) *Glycobiology* 14(2), 103-114
31. O'Neil, K. T., and DeGrado, W. F. (1990) *Science* 250(4981), 646-651
32. Jenke, M., Sanchez, A., Monje, F., Stuhmer, W., Weseloh, R. M., and Pardo, L. A. (2003) *Embo J* 22(3), 395-403
33. Napp, J., Monje, F., Stuhmer, W., and Pardo, L. A. (2005) *J Biol Chem* 280(33), 29506-29512
34. Much, B., Wahl-Schott, C., Zong, X., Schneider, A., Baumann, L., Moosmang, S., Ludwig, A., and Biel, M. (2003) *J Biol Chem* 278(44), 43781-43786
35. Hendriks, G., Koudijs, M., van Balkom, B. W., Oorschot, V., Klumperman, J., Deen, P. M., and van der Sluijs, P. (2004) *J Biol Chem* 279(4), 2975-2983
36. Chang, Q., Hoefs, S., van der Kemp, A. W., Topala, C. N., Bindels, R. J., and Hoenderop, J. G. (2005) *Science* 310(5747), 490-493
37. Owsianik, G., Talavera, K., Voets, T., and Nilius, B. (2006) *Annu Rev Physiol* 68, 685-717

FOOTNOTES

While this manuscript was in revision, Dragoni et al (J Biol Chem, online edition Oct. 2) published a study analyzing the role of the double cysteine motif within the pore loop of TRPM8. In this study the authors also investigate the relevant glycosylation site. Concerning the role of N-linked glycosylation at N934, the authors come to similar conclusions as our study.

We thank Dr. Miesenbock for kindly providing us with the cDNA for the superecliptic pH-sensitive GFP, Sabrina Ploog, Katja Schuster, Thomas Aberle and Heidi Löhr for technical assistance and cell culture work and members of the lab for critical input. This work was supported, in part, by the Deutsche Forschungsgemeinschaft (B.N.: NI 671), HOMFOR (B.N.) and Sander-Stiftung (V.F.). D.A-A. is a member of the DFG sponsored graduate program GK 1326.

The abbreviations used are: HEK-293, human embryo kidney-293; SEM, standard error of the mean; TRP, transient receptor potential;

FIGURE LEGENDS

Fig: 1**.** *A.* Schematic representation of hTRPM8 constructs tested in the Bacteriomatch® II hybrid system. *B.* Results from the interaction analysis. pBTL and pTRP are the bait- and target vectors with the inserted TRPM8 fragments. The strength of interaction was detected by counting the colonies and was defined as follows: negative (-) < 100 colonies, + > 100 colonies, ++ > 300 colonies, +++ > 1000 colonies. pBT-LGF2 amd pTRG-Gal11 were positive controls (Stratagene) that were included in each round of electroporation.

Fig. 2. *A.* Schematic representation of hTRPM8 constructs with a C-terminal pH sensitive GFP variant S-pHluorin (SpH) tag used in co-immunprecipitation experiments. Putative coiled-coil regions 1, 2, 3 and 4 are indicated; black boxes indicate predicted transmembrane segments (TM) 1 to 6; C-terminal SpH tag is indicated by the green box. *B.* Protein-interaction analysis after expression of the tagged constructs in stable TRPM8 expressing cells. Each fusion protein was expressed at its expected molecular weight (TRPM8-SpH: 154 kDa, NT-SpH: 106 kDa, N3-SpH: 87 kDa, Δ-CT-SpH: 133 kDa) and the amount of fusion protein precipitated with the anti-GFP antibody and bound to sepharose-G beads was dectected using anti-GFP antibody. The ability to co-precipitate wild-type TRPM8 was analyzed by detecting untagged TRPM8 (128 kDa) in the protein-G bound fraction using the polyclonal anti-TRPM8 antibody. The unbound fractions were checked for equal expression levels of endogenous TRPM8 by detection with anti-TRPM8. *C.* Results of the two-hybrid analysis after mutating L1089P within the pBTL-CT construct. *D.* Corresponding results after immunprecipitation of full-length TRPM8 L1089P. Arrows in *B* and *D* point to the non-glycosylated (black arrows) and to the complex glycosylated (red arrows) form of endogenous TRPM8 (127 kDa) and of TRPM8-SpH fusion protein (~150 kDa). E. Current-voltage relationship of transiently expressed EYFP-TRPM8 and EYFP-TRPM8 L1089P after stimulation with 100 µM menthol in bath solution. Inset shows time course of menthol response at -101 mV and +31 mV ramp potential. *F*. Surface biotinylation of TRPM8-SpH and TRPM8-L1089-SpH. A: 1/3 of total avidin bound fraction, S: 50 µg protein of unbound fraction.

Fig. 3. *A.* Mutating the CC region alters the ability of EYFP tagged TRPM8 to form multimers. Immunoblot (anti-TRPM8) analyses of fractions after centrifugation on a 15-25% sucrose gradient. The fractions with peak intensities of marker protein (thyroglobulin 670 kDa, ferritin, 440 kDa, catalase, 240 kDa, ß-galactosidase 116 kDa) are indicated above. Blots were stripped and reprobed with an anti-IP3RIII antibody and the peak fraction is indicated by the 1200 kDa arrow. *B.* Dominant-negative effect on wild-type menthol induced current changes after cotransfection of EYFP-TRPM8 with either pEYFP vector (EYFP), EYFP-CT (CT), EYFP–TM6-CT (TM6-CT) or EYFP-TM6-CTΔ1088-1104 (TM6-CTΔ). Currents were analyzed at -101 mV and at +51 mV ramp potential. *p< 0.05; ** p< 0.01, *** p< 0.001, statistics for outward currents. *C.* Dominant negative effects on endogenous TRPM8 (stable cell line, wt) currents after expression of EYFP-CT (CT), EYFP–TM6-CT (TM6-CT), EYFP-TM6-CT L1089P (TM6-CT L/P) or full length EYFP-TRPM8 L1089P (L/P). *D.* Co-immunoprecipitation of untagged wild-type TRPM8 with TM6-CT*-SpH (aa 911-1104; ~ 49,6 kDa) and with CT-SpH (aa 978-1104, ~ 41,5 kDa). Protein-G bound input above and detected with anti-GFP, Western blot of IP and 50 µg unbound supernatant with anti-TRPM8. *E.* Western blot of

TM6-CT*-SpH or N934Q TM6-CT*-SpH expressing HEK 293 cell lysates. Western blot was probed with anti-TRPM8 antibody.

Fig. 4. Role of posttranslational modification by N-linked glycosylation. *A.* 50 µg of microsomal protein preparations from HEK-TRPM8 cells were treated either with Endoglycosidase H or with Ngase F, resolved on SDS-PAGE gels and detected with anti-TRPM8. *B.* Putative transmembrane topology of TRPM8. Blue elliptic structures indicate hydrophobic domains, red branches indicate the location of potential N-linked glycosylation sites. *C.* Western blot analysis of EYFP tagged wild-type and EYFP tagged glycosylation-site mutants. *D.* Surface biotinylation of EYFP-wt, EYFP-N934Q and EYFP-N934Q_H946N. A: Avidin bound fraction, S: 50 µg unbound fraction. Detection with anti-GFP antibody.

Fig. 5. *A.* Time course of menthol (100 µM) invoked inward and outward currents for EYFP-TRPM8 (black) and EYFP-N934Q-TRPM8 (gray). *B.* Sample current-voltage relationships for an EYFP-tagged TRPM8 wild-type (black) and non-glycosylated TRPM8-N934Q mutant (gray). *C.* Quantification of Menthol induced changes in current densities (pA/pF) at -101 mV and +31 mV ramp potential for TSA cells transfected with EYFP-tagged wild-type, N934Q, H946N and N934Q-H946N TRPM8. *D.* Co-Immunprecipitation of untagged wild-type TRPM8 with TRPM8-N934Q-SpH. S: 50 µg unbound supernatant.

Supplementary Data

Fig. S1. Alignment of human TRPM coiled-coil regions.

Figure 1

A

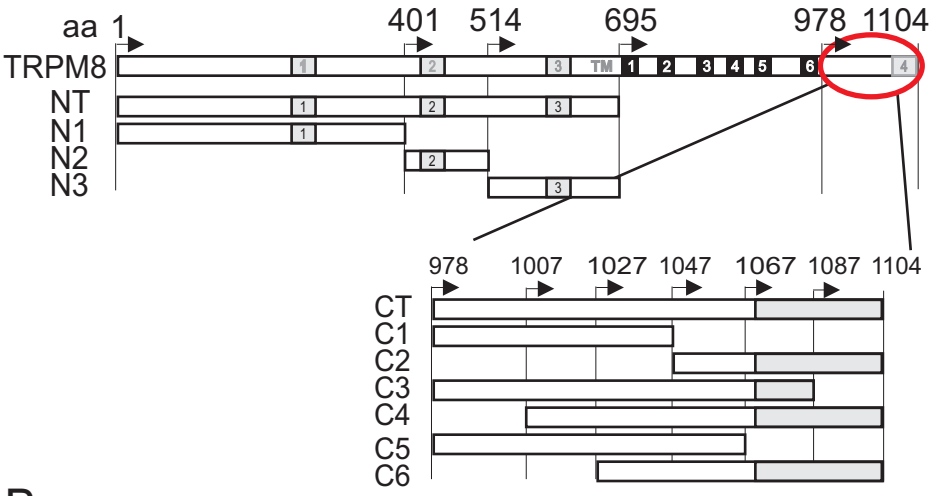

B

pBTL	aa	pTRG		interaction
NT	1-694	NT	1-694	-
		N1	1-400	-
		CT	978-1104	-
N2	401-513	NT	1-694	-
		N1	1-400	-
		N2	401-513	+
		N3	514-694	-
		CT	978-1104	++
N3	514-694	NT	1-694	-
		N1	1-400	+
		N3	514-694	+++
		CT	978-1104	++
CT	978-1104	CT	978-1104	+++
		C1	978-1046	-
		C3	978-1086	-
C2	1047-1104	CT	978-1104	+
C4	1007-1104	CT	978-1104	+++
		C3	978-1086	-
		C5	978-1066	-
C6	1027-1104	CT	978-1104	++
		C3	978-1086	-
		C5	978-1066	-
pBTL		all TRPM8 pTRG constructs		-
all TRPM8 pBTL constructs		pTRG		-
pBT-LGF		pTRG-Gal11P		+++

Figure 2

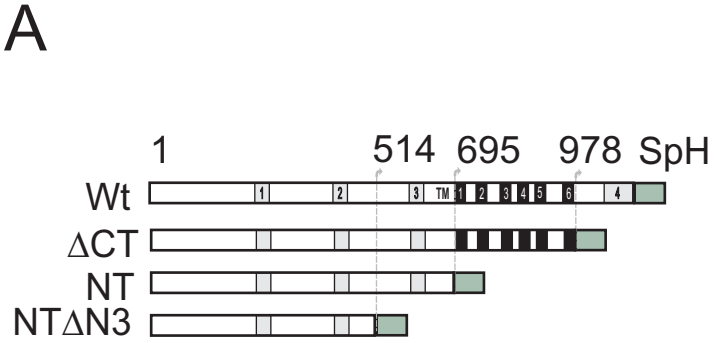

C

pBTL	pTRG	interaction
CT 978-1104	CT	+++
CT L1089P	CT	-

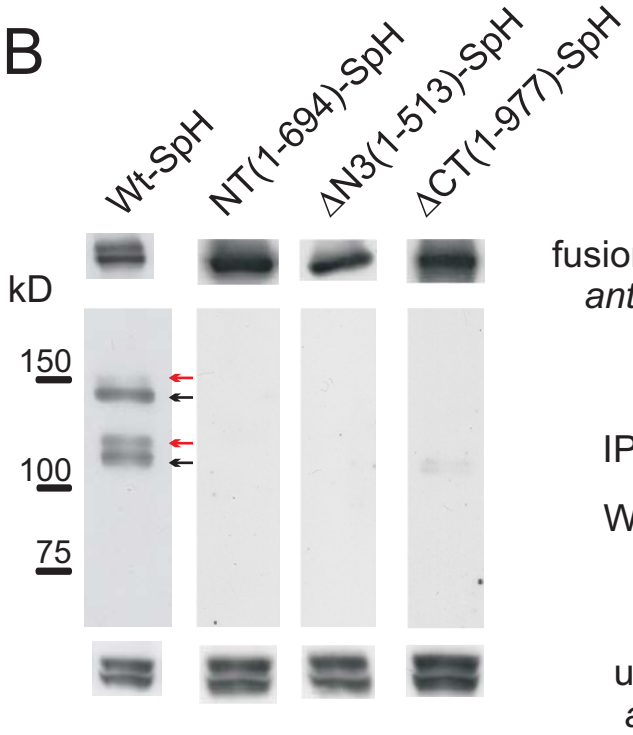

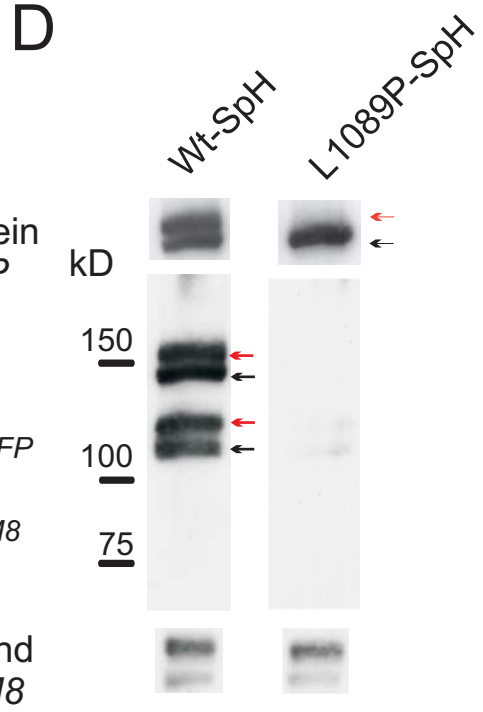

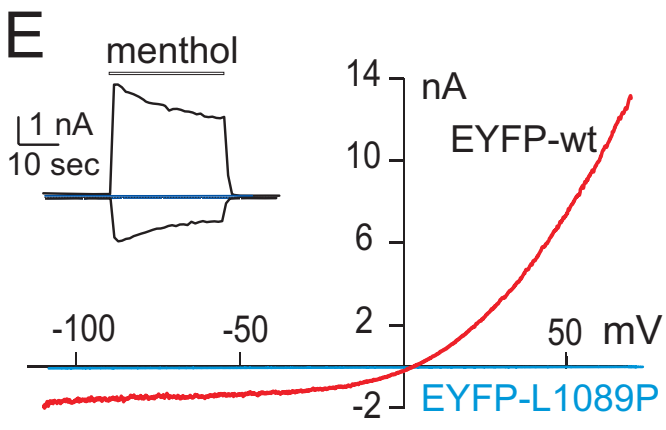

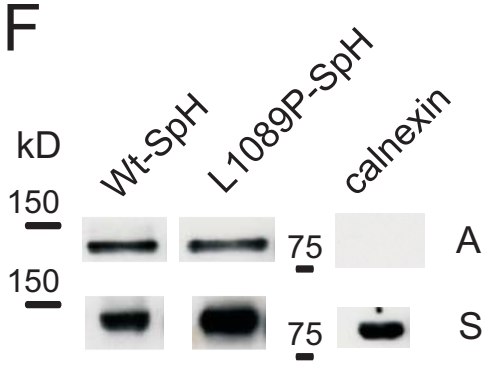

Figure 3

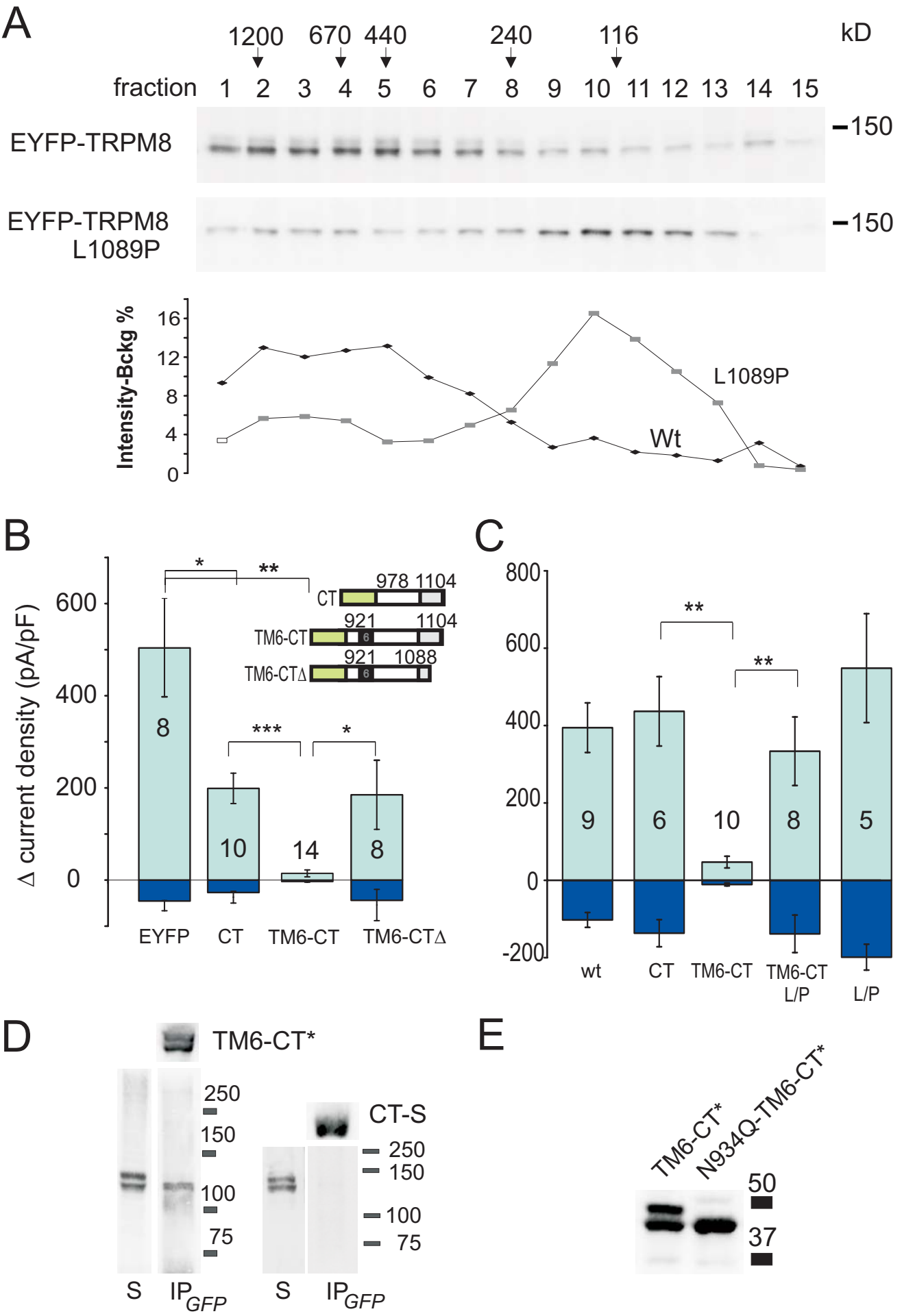

Figure 4

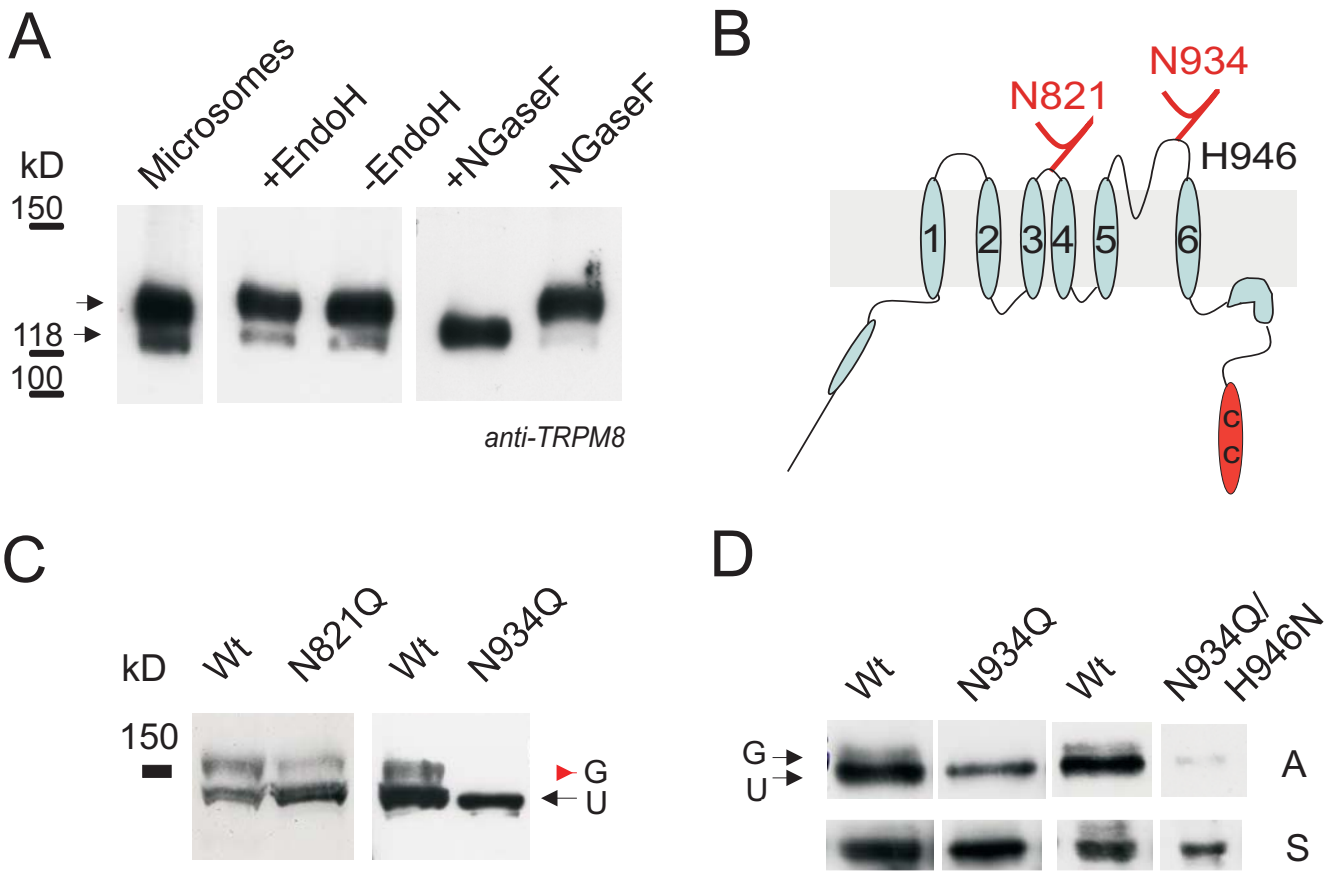

Figure 5

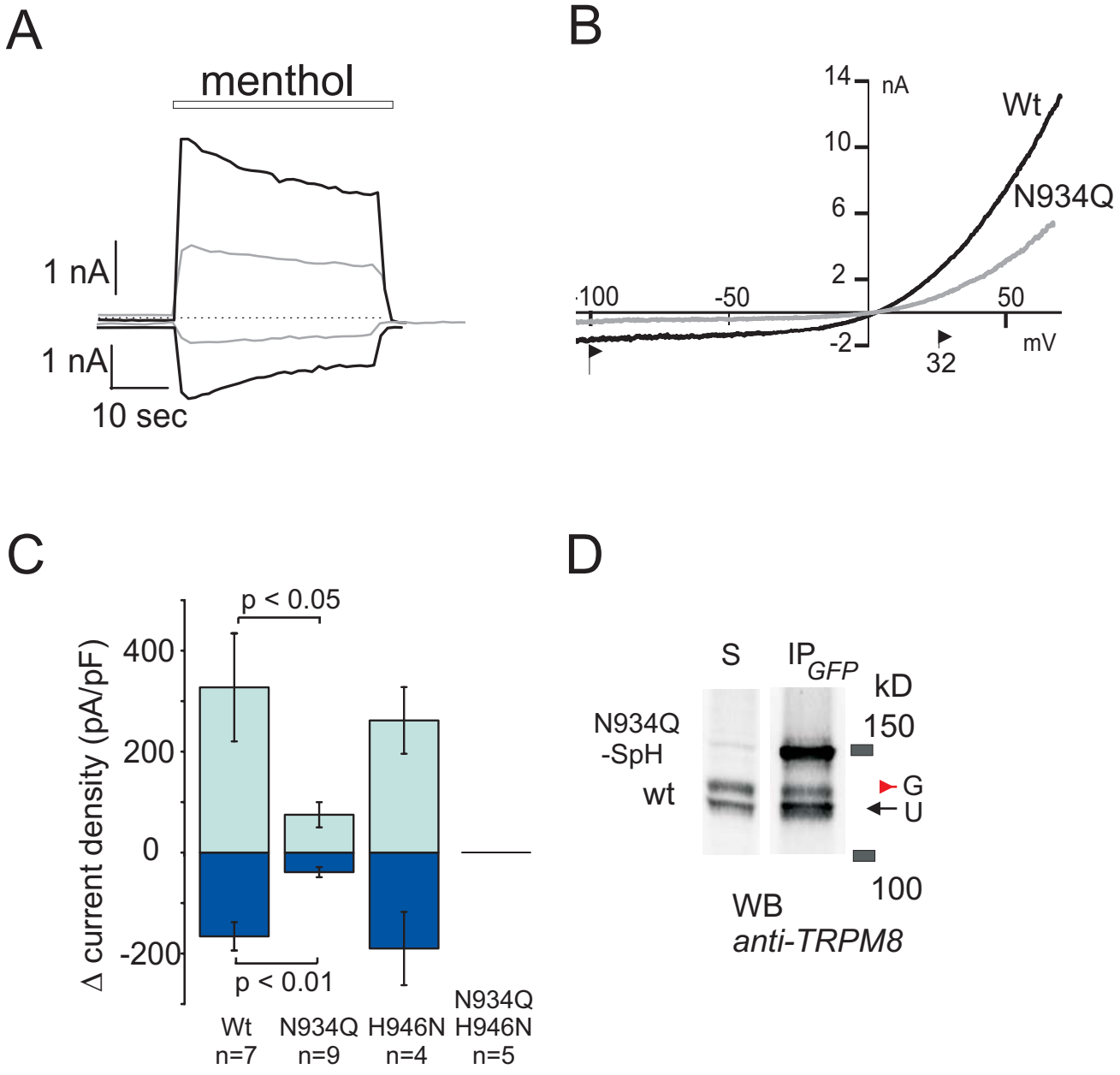

Figure S1

A

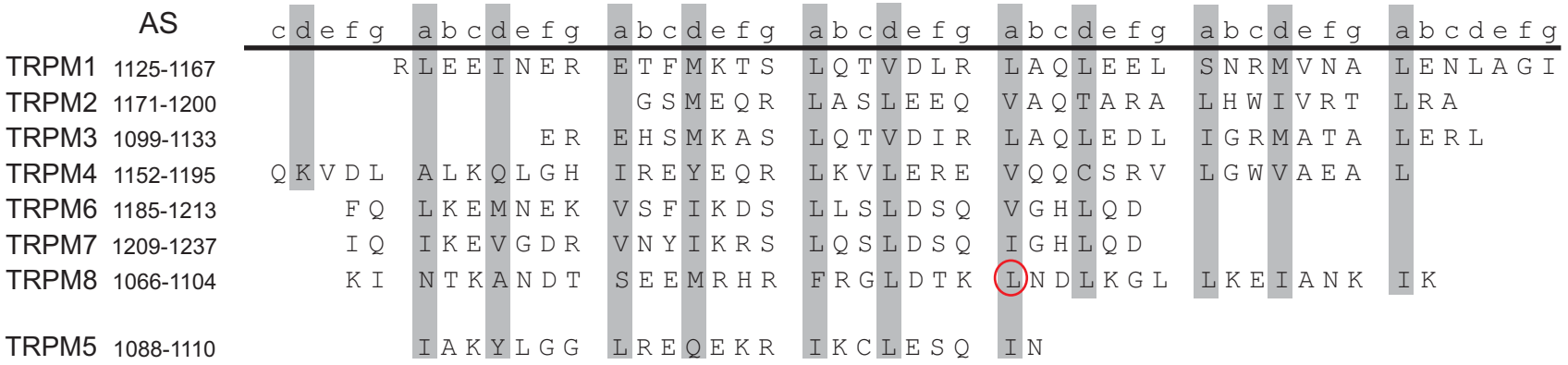

B

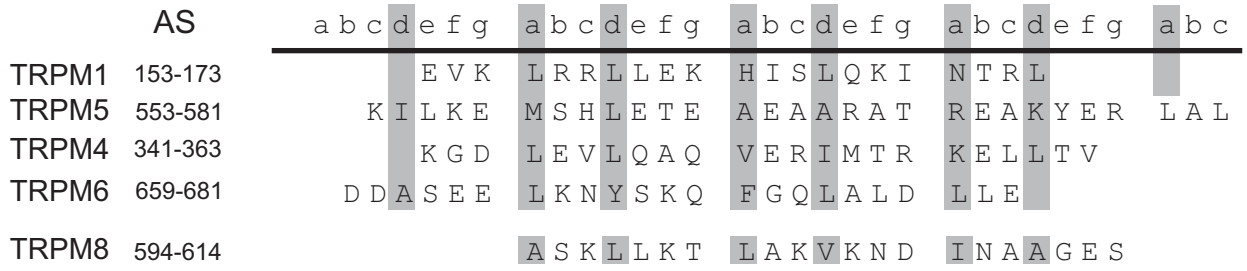

Fig. S1. Alignment of human TRPM coiled-coil regions. *A.* Shown are potential C-terminal coiled-coil (CC) regions that show a high probability (> 50%) of forming a four-heptad coiled-coil structure after calculation with a 2.5 weighted probability of hydrophobic amino acids in positions *a* and *d* (27). For the C-terminal CC region of TRPM5 a probability of > 50 % could only be obtained for a three-heptad CC region. *B.* Potential N-terminal three-heptad coiled-coil regions with a weighted probability > 50%. TRPM5 is the only member with a high probability of forming a four-heptad N-terminal CC region. TRPM8 has a single N-terminal three heptad CC region, however with a probability of only 44 %.

Trafficking and assembly of the cold-sensitive TRPM8 channel

Isabell Erler, Dalia M.M. Al-Ansary, Ulrich Wissenbach, Thomas F.J. Wagner, Veit Flockerzi and Barbara A. Niemeyer

J. Biol. Chem. published online October 25, 2006
